Applied Acoustics 211 (2023) 109463

Contents lists available at ScienceDirect

Applied Acoustics

journal homepage: www.elsevier.com/locate/apacoust

Power flow sensitivity analysis for optimal structural modification

J.W.R. Meggitt

Acoustics Research Centre, University of Salford, Greater Manchester, M5 4WT, United Kingdom

ARTICLE INFO

Article history:
Received 5 March 2023
Received in revised form 25 April 2023
Accepted 26 May 2023

Keyword:
Power flow
Structural modification
Blocked force
Noise control

ABSTRACT

Across many industries there is a need to develop products with improved vibro-acoustic performance. Whether the aim is to reduce the radiated sound level in a vehicle cabin, or to minimise the vibration level of sensitive components, the problem may be interpreted as an issue of power transmission from vibration generating components to receiving structures. Interest thus lies in how best to modify a structure, typically the separating interface between active and passive components, to reduce transmitted power. The 'best' modification is interpreted here as the one that achieves the greatest reduction in transmitted power, for the smallest necessary modification. In the present paper we consider power transmission from a component-based perspective, and propose a sensitivity analysis to determine a) the optimum structural modifications (e.g. added mass, stiffness or damping) and b) to which degrees of freedom these should be applied. Numerical and experimental examples demonstrate the proposed method.

1. Introduction

The optimisation of dynamic structures for improved vibro-acoustic performance is prevalent in many sectors. Whether the aim is to reduce the radiated sound level in a vehicle cabin, or to minimise the vibration level of sensitive components, the problem can be interpreted as an issue of vibrational power flow from the generating component to the remaining structure. By reducing the power flow from an active component (i.e. one that generates vibration, e.g. pumps, motors, etc.) to a passive receiver (i.e. one that simply transmits or radiates vibration), the available energy that can excite the structure is reduced, thereby reducing the overall downstream response level.

As a quantity, power flow is a convenient variable to deal with when tackling structural vibration problems. Complex interface dynamics, represented by many degrees of freedom (DoFs, including translational and rotational motions), are simplified to a single frequency dependent scalar quantity. This can greatly simplify and aid the interpretation of complex transmission problems.

The study of power transmission through built-up structures has received much attention over the past decades, see for example the notable works in [1–7]. Though, in recent years attention has turned towards more flexible/detailed methods that are able to provide greater information on the propagation of vibration through a structure, for example, the class of methods known widely as Transfer Path Analysis (TPA) [8]. This transition from power-based methods, to more detailed analyses has been driven largely by the availability of multi-channel acquisition systems and the necessary computational power to process collected data, but also the need to solve ever more challenging problems. Nevertheless, power-based methods remain a valuable tool for the analysis of complex structures and form the basis of many techniques still used today, for example Statistical Energy Analysis (SEA) [9] and its various extensions [10,11].

This paper concerns the use of power flow sensitivity to identify optimum structural modifications. A power-based approach is chosen as it simplifies the interface problem and thus provides a more interpretable analysis. Our starting point is the equation for time averaged complex power flow $Q \in \mathbb{C}$ through a structural interface c,

$$Q = \frac{1}{2}\mathbf{g}_c^{\mathrm{H}}\mathbf{v}_c \tag{1}$$

where: $\mathbf{g}_c \in \mathbb{C}^N$ is the contact force imparted on the receiver structure by a vibrating source, $\mathbf{v}_c \in \mathbb{C}^N$ is the coupled assembly velocity whilst the source is operational, and $\square^{\mathrm{H}}$ is the Hermitian transpose operator. From Eq. 1 it is clear that the power flow through an interface is dependent on two factors: the strength of the source, and the transmission characteristics of the source-receiver interface c.

We are interested in determining the optimum (i.e. the most efficient) modification of a structure to reduce the power flow Q. This optimum modification should provide the greatest reduction in transmitted power, for the smallest change in the dynamic properties of the structure (e.g. added mass, stiffness or damping). This '*optimum*' modification is beneficial in cases where design changes

https://doi.org/10.1016/j.apacoust.2023.109463
0003-682X/

must be kept to a minimum, for example to avoid influencing other key performance characteristics (e.g. handling/comfort in an automotive case) or costly redesigns.

To achieve an optimum modification it is necessary to determine a) *what sort* of structural modification should be applied and b) to *what part* of the structure. The above is made possible by two sensitivity relations, which represent the partial derivatives of the transmitted power with respect to reactive (added mass or stiffness) and resistive (added damping) structural modifications (i.e. change of the receiver structure's impedance); $\frac{\partial \Re(Q)}{\partial \Im(Z_R)}$ and $\frac{\partial \Re(Q)}{\partial \Re(Z_R)}$ (see Eq. 27 and 28).

In the present paper, these relations are derived in a *component-based* form, i.e. based on measurements of the source and receiver components in isolation. By implementing these relations, it is possible to identify not only the optimum DoFs to modify, but also the type of modification necessary to achieve the greatest reduction in transmitted power across a target frequency range. The derivation, interpretation and application of these power flow sensitivity relations is the primary result of this paper.

Methods for obtaining an optimal structural modification for improved vibro-acoustic performance have long been researched. Methods generally differ in what metric is used to quantify vibro-acoustics performance, and whether passive [12,13] or active [14,15] modifications are considered. Typical performance metrics include power flow [14,15,13] and structural admittance [16,17,12]. The most closely related work to that presented here is the power flow sensitivity analysis described in [18]. The approach proposed herein differs in two main respects. 1) In the present study, vibration source activity is represented by the blocked force [19], as opposed to free velocity or the assembly interface force. This is advantageous as the blocked force has become an internationally recognised standard for vibration source characterisation [20]-, and is used widely across various industries (notably the automotive sector as part of insitu [21] and component-based TPA [8]). 2) The inclusion of distributed modifications (i.e. adding stiffness or damping between non-collocated DoFs) is treated more carefully; in [18] only the influence of off-diagonal impedance terms where considered, herein we consider also the effect of the diagonal elements of the impedance matrix.

Having introduced the context of this paper, its remainder will be organised as follows. Section 2 will outline some underlying theory, specifically the concepts of blocked force and complex power. Section 3 will go on to derive power flow sensitivity relations (Eqs. 25 and 26) for both local and distributed modifications. Section 4 will present a numerical study for verification and investigatory purposes. An experimental study will be presented in Section 5 before Section 6 draws some concluding remarks.

2. Theory

This section will begin by introducing the blocked force approach to vibratory source characterisation before a component-based representation of complex power is introduced.

2.1. Blocked force

In its standard form, the complex power (see Eq. 1) is formulated in terms of the contact force $\mathbf{g}_c$. The contact force is dependent on both the activity of the vibratory source, and the dynamics of the receiver structure. This means that a change in either the source or receiver will alter the contact force. Consequently, Eq. 1 is not suitable for investigating the power flow in 'virtual assemblies', i.e. where components are interchanged in search for an optimal design. We are interested in reformulating the complex power such that it is expressed in terms of component level quantities, enabling it to be used in a virtual prototyping context. To do so we must introduce appropriate descriptions of the assemblies active and passive properties. With regards to the active properties, the blocked force provides an appropriate description.

The blocked force is a quantity that independently describes the activity of a vibration source. It is an invariant source quantity that is unaffected by the dynamics of neighbouring components.

The blocked force may be interpreted as the force required to constrain the interface of a vibration source such that its velocity (also displacement and acceleration) is zero. Alternatively, it may be thought of as the force imparted by an infinitely rigid receiver onto an operating vibration source. It is defined as,

$$\bar{\mathbf{f}}_c = \mathbf{g}_c|_{\mathbf{v}_c=0} \tag{2}$$

where the over-bar $\bar{\square}$ is used to denote a *blocked* force, as opposed to an external force.

In recent years, the blocked force has become a popular means of characterising vibration sources. Its popularity has been spurred by the development of an in-direct method for its characterisation [19], which avoids the challenging experimental requirements of a direct measurement. The key equation behind a blocked force characterisation is [19],

$$\mathbf{v}_b = \mathbf{Y}_{Cbc}\bar{\mathbf{f}}_c \tag{3}$$

where: $\mathbf{Y}_{Cbc} \in \mathbb{C}^{M\times N}$ is the measured transfer mobility matrix of the coupled (C) assembly, $\mathbf{v}_b \in \mathbb{C}^M$ is a measured operational velocity vector (note that accelerance and acceleration may be used in place of mobility and velocity), and $\bar{\mathbf{f}}_c \in \mathbb{C}^N$ is the vector of unknown blocked forces. Here, lower-case subscripts b and c represent remote receiver and coupling interface DoFs, respectively (see Fig. 1). Note that the DoF set b may include the interface DoFs c as a subset and that all variables are represented in the frequency domain, with the frequency variable omitted for clarity.

Eq. 3 can be solved for the blocked force by inverting the measured mobility matrix. For $N = M$, providing that the measured mobility matrix is of full rank, a unique solution is found through the inverse mobility matrix $\mathbf{Y}^{-1}_{Cbc} = \mathbf{Z}_{Ccb}$, where $\mathbf{Z}_{Ccb} \in \mathbb{C}^{N\times N}$ is an assembly impedance matrix. For $M > N$, the pseudo-inverse may be used in place of the classical matrix inverse to obtain $\mathbf{Y}^{+}_{Cbc} = \mathbf{Z}_{Ccb} \in \mathbb{C}^{M\times N}$, leading to a least squares solution of the problem. It is important when characterising the blocked force that a complete interface description is used [22–24], i.e. a sufficient number of DoFs are chosen at the interface c. If the interface description is incomplete, the blocked force may no longer be transferred between assemblies and used to predict the vibro-acoustic response in a new assembly. It is also important that the chosen indicator DoFs b are suitable, such that they are able to maximally observe the interface dynamics. A criterion for choosing indicator sensor positions is proposed in [25].

Finally, it is important to note that the characterisation of blocked force is an inverse problem. Inverse problems can be sensitive to experimental error, and so an appropriate uncertainty propagation maybe be necessary. A framework for propagating experimental and source-based uncertainty through a blocked force characterisation may be found in [26].

In the present paper we will use the blocked force to describe the activity of a vibration source when considering vibrational power transmitted through an interface.

2.2. Complex power

For a multi-contact system undergoing time harmonic motion, the time averaged complex power Q is defined as [27],

$$Q = \frac{1}{2}\mathbf{g}_c^{\mathrm{H}}\mathbf{v}_c \tag{4}$$

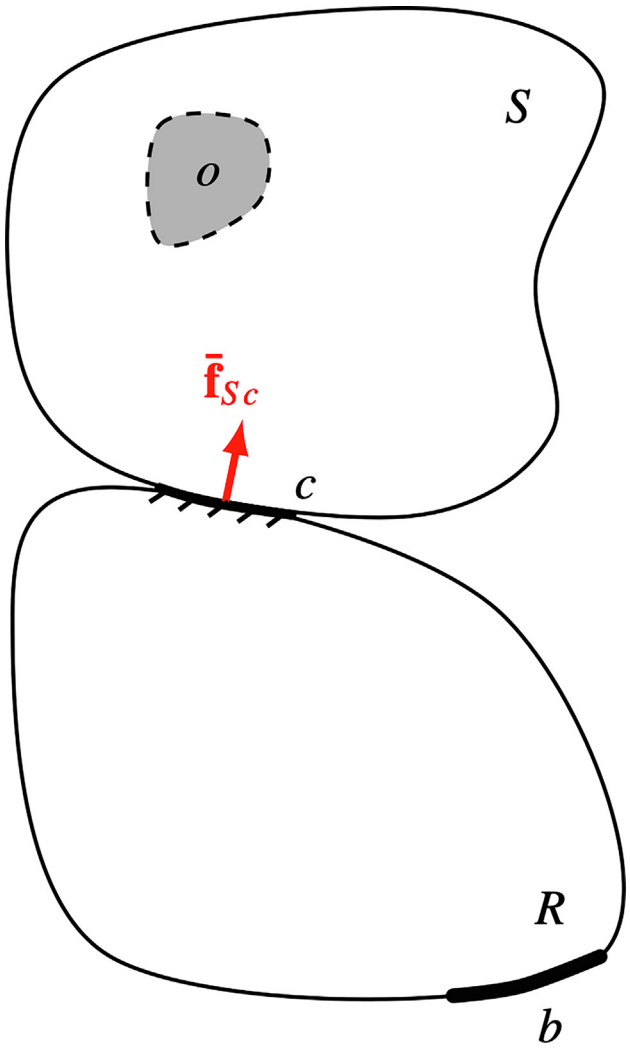

Fig. 1. Diagrammatic representation of source-receiver (SR) assembly and blocked force.

where, $\mathbf{g}_c$ is the interface contact force imparted on a receiver structure by the vibration source, $\mathbf{v}_c$ is the interface velocity of the coupled assembly, and $\square^{\mathrm{H}}$ represents the conjugate transpose operation.

Unlike the contact force or interface velocity, the complex power is a scalar value. This can be advantageous when dealing with complex interface dynamics, as problem reduces to a single value which can more easily be interpreted.

The real part of complex power describes the power transmitted into the receiver structure and away from the interface. It is this transmitted power that is proportional to the observed vibration levels in the receiver structure and of principle interest in noise control applications. The imaginary part of complex power describes the power that oscillates between kinetic and potential, and remains 'trapped' at the interface. In the context of noise control, the oscillating power is typically of little interest [6].

We are interested in reformulating Eq. 4 in terms of component level quantities (for clarity we omit the factor of $1/2$ hereafter). To do so we begin by expressing the coupled velocity in terms of the blocked force $\bar{\mathbf{f}}_c$,

$$Q = \mathbf{g}_c^{\mathrm{H}} \mathbf{Y}_{Ccc} \bar{\mathbf{f}}_c. \tag{5}$$

Next we substitute the contact force $\mathbf{g}_c$ for its inverse relation to the coupled velocity,

$$Q = \left(\mathbf{Y}_{Rcc}^{-1}\mathbf{v}_c\right)^{\mathrm{H}} \mathbf{Y}_{Ccc}\bar{\mathbf{f}}_c = \mathbf{v}_c^{\mathrm{H}}\mathbf{Y}_{Rcc}^{-\mathrm{H}}\mathbf{Y}_{Ccc}\bar{\mathbf{f}}_c. \tag{6}$$

The coupled velocity can again be expressed in terms of the blocked force,

$$Q = \left(\mathbf{Y}_{Ccc}\bar{\mathbf{f}}_c\right)^{\mathrm{H}}\mathbf{Y}_{Rcc}^{-\mathrm{H}}\mathbf{Y}_{Ccc}\bar{\mathbf{f}}_c = \bar{\mathbf{f}}_c^{\mathrm{H}}\mathbf{Y}_{Ccc}^{\mathrm{H}}\mathbf{Y}_{Rcc}^{-\mathrm{H}}\mathbf{Y}_{Ccc}\bar{\mathbf{f}}_c. \tag{7}$$

Noting that the coupled mobility $\mathbf{Y}_C = [\mathbf{Y}_S^{-1} + \mathbf{Y}_R^{-1}]^{-1}$ may readily be expressed in terms of the source and receiver mobilities, Eq. 7 describes the complex power Q in terms of component level quantities, i.e. the receiver mobility $\mathbf{Y}_R$, the source mobility $\mathbf{Y}_S$, and the blocked force $\bar{\mathbf{f}}_c$.

In contrast to its standard form (see Eq. 4), Eq. 7 now facilitates the virtual interchange of components. In the following section Eq. 7 will be used to derive a sensitivity relation for the power flow through an interface due to a structural modification within the receiver structure.

3. Power flow sensitivity

The focus of this section is to derive Eqs. 25 and 26, which describe the sensitivity of transmitted power to a local or distributed structural modification of the receiver structure.

Whilst modifications at the coupling interface might be expected to result in the greatest change in transmitted power, in practice such modifications may not be possible, hence remote DoFs away from the interface should also be considered. To enable modifications made remote from the interface, i.e. within the receiver, it is convenient to define interfacial power in terms of the global force and velocity vectors, $\mathbf{g}$ and $\mathbf{v}$. The interface contact force and velocity can be related to the global force and velocity vectors by the selection matrices $\mathbf{S}_v$ and $\mathbf{S}_f$,

$$\mathbf{v}_c = [\mathbf{I} \quad \mathbf{0}]\begin{pmatrix}\mathbf{v}_c \\ \mathbf{v}_b\end{pmatrix} = \mathbf{S}_v\mathbf{v}, \tag{8}$$

$$\mathbf{g}_c = [\mathbf{I} \quad \mathbf{0}]\begin{pmatrix}\mathbf{g}_c \\ \mathbf{g}_b\end{pmatrix} = \mathbf{S}_f\mathbf{g}. \tag{9}$$

Using the above, the equation for complex power becomes,

$$Q = \mathbf{g}^{\mathrm{H}}\mathbf{S}\mathbf{v} \tag{10}$$

with $\mathbf{S} = \mathbf{S}_f^{\mathrm{T}}\mathbf{S}_v$, or in component form,

$$Q = \bar{\mathbf{f}}^{\mathrm{H}}\mathbf{Y}_C^{\mathrm{H}}\mathbf{Y}_R^{-\mathrm{H}}\mathbf{S}\mathbf{Y}_C\bar{\mathbf{f}} \tag{11}$$

where $\mathbf{Y}_R$ and $\mathbf{Y}_C$ are now extend to include remote DoFs alongside those at the interface, and the blocked force vector $\bar{\mathbf{f}} = [\bar{\mathbf{f}}_c^{\mathrm{T}} \quad \mathbf{0}^{\mathrm{T}}]^{\mathrm{T}}$ is zero-padded accordingly.

To obtain a power sensitivity relation wrt. a structural modification, we begin by taking the complex differential of Eq. 11,

$$d(Q) = d\left(\bar{\mathbf{f}}^{\mathrm{H}}\mathbf{Y}_C^{\mathrm{H}}\mathbf{Y}_R^{-\mathrm{H}}\mathbf{S}\mathbf{Y}_C\bar{\mathbf{f}}\right). \tag{12}$$

Note that a structural modification alters the receiver mobility $\mathbf{Y}_R$ which in turn alters the coupled mobility $\mathbf{Y}_C$. The source mobility and blocked force are unaffected as they are invariant to the receiver structure.

Applying the chain rule to Eq. 12, noting that interest lies in the differential receiver mobility/impedance, yields,

$$\begin{aligned} d(Q) = \quad & \bar{\mathbf{f}}^{\mathrm{H}}d\left([\mathbf{Z}_R + \mathbf{Z}_S]^{-\mathrm{H}}\right)\mathbf{Y}_R^{-\mathrm{H}}\mathbf{S}\mathbf{Y}_C\bar{\mathbf{f}} + \bar{\mathbf{f}}^{\mathrm{H}}\mathbf{Y}_C^{-\mathrm{H}}d\left(\mathbf{Z}_R^{\mathrm{H}}\right)\mathbf{S}\mathbf{Y}_C\bar{\mathbf{f}} + \cdots \\ & \bar{\mathbf{f}}^{\mathrm{H}}\mathbf{Y}_C^{-\mathrm{H}}\mathbf{Y}_R^{-\mathrm{H}}\mathbf{S}d\left([\mathbf{Z}_R + \mathbf{Z}_S]^{-1}\right)\bar{\mathbf{f}} \end{aligned} \tag{13}$$

where we have substituted $\mathbf{Y}_C = (\mathbf{Z}_R + \mathbf{Z}_S)^{-1}$ and $\mathbf{Y}_R^{-1} = \mathbf{Z}_R$ for the differential terms. Assuming that the coupled impedance matrix is

square and its inverse exists, its complex differential can be re-written as [28],

$$\begin{aligned} d\left([\mathbf{Z}_R+\mathbf{Z}_S]^{-1}\right) &= -\mathbf{Y}_C d(\mathbf{Z}_R+\mathbf{Z}_S)\mathbf{Y}_C \\ &= -\mathbf{Y}_C d(\mathbf{Z}_R)\mathbf{Y}_C. \end{aligned} \tag{14}$$

Noting that $d(\mathbf{A}^{\mathrm{H}}) = d(\mathbf{A})^{\mathrm{H}}$ [28] and substituting the above into Eq. 13, yields,

$$\begin{aligned} d(Q) = \; & -\bar{\mathbf{f}}^{\mathrm{H}}\mathbf{Y}_C^{\mathrm{H}} d\left(\mathbf{Z}_R^{\mathrm{H}}\right)\mathbf{Y}_C^{\mathrm{H}}\mathbf{Y}_R^{-\mathrm{H}}\mathbf{S}\mathbf{Y}_C\bar{\mathbf{f}} + \bar{\mathbf{f}}^{\mathrm{H}}\mathbf{Y}_C^{-\mathrm{H}} d\left(\mathbf{Z}_R^{\mathrm{H}}\right)\mathbf{S}\mathbf{Y}_C\bar{\mathbf{f}} - \cdots \\ & \bar{\mathbf{f}}^{\mathrm{H}}\mathbf{Y}_C^{-\mathrm{H}}\mathbf{Y}_R^{-\mathrm{H}}\mathbf{S}\mathbf{Y}_C d(\mathbf{Z}_R)\mathbf{Y}_C\bar{\mathbf{f}} \end{aligned} \tag{15}$$

which after factoring out repeated terms simplifies to,

$$d(Q) = \bar{\mathbf{f}}^{\mathrm{H}}\mathbf{Y}_C^{\mathrm{H}}\left(-d\left(\mathbf{Z}_R^{\mathrm{H}}\right)\mathbf{Y}_C^{\mathrm{H}}\mathbf{Y}_R^{-\mathrm{H}}\mathbf{S} + d\left(\mathbf{Z}_R^{\mathrm{H}}\right)\mathbf{S} - \mathbf{Y}_R^{-\mathrm{H}}\mathbf{S}\mathbf{Y}_C d(\mathbf{Z}_R)\right)\mathbf{Y}_C\bar{\mathbf{f}}. \tag{16}$$

Note that $d(\mathbf{Z}_R)$ represents a small (complex) change in each element of the receiver impedance matrix $\mathbf{Z}_R$, i.e. due to an infinitesimal structural modification.

The structural modifications considered here can be described as; local, where added mass or grounded stiffness/damping is applied to a single DoF; or distributed, where added stiffness or damping is applied between two DoFs. For a local modification, $d(\mathbf{Z}_R)$ reduces to a single entry matrix,

$$\begin{aligned} d(\mathbf{Z}_R) &= \begin{bmatrix} 0 & 0 & 0 & 0 \\ 0 & 0 & 0 & 0 \\ 0 & 0 & d(Z_R) & 0 \\ 0 & 0 & 0 & 0 \end{bmatrix} \\ &= \begin{bmatrix} 0 & 0 & 0 & 0 \\ 0 & 0 & 0 & 0 \\ 0 & 0 & 1 & 0 \\ 0 & 0 & 0 & 0 \end{bmatrix} d(Z_R) \\ &= \mathbf{P}_{ii} d(Z_R) \end{aligned} \tag{17}$$

where $d(Z_R)$ takes, in general, the form,

$$d(Z_R) = d\left(R + i\omega M + \frac{K}{i\omega}\right). \tag{18}$$

For a distributed modification,

$$\begin{aligned} d(\mathbf{Z}_R) &= \begin{bmatrix} 0 & 0 & 0 & 0 \\ 0 & d(Z_R) & -d(Z_R) & 0 \\ 0 & -d(Z_R) & d(Z_R) & 0 \\ 0 & 0 & 0 & 0 \end{bmatrix} \\ &= \begin{bmatrix} 0 & 0 & 0 & 0 \\ 0 & 1 & -1 & 0 \\ 0 & -1 & 1 & 0 \\ 0 & 0 & 0 & 0 \end{bmatrix} d(Z_R) \\ &= \mathbf{P}_{ij} d(Z_R) \end{aligned} \tag{19}$$

where $\mathbf{P}_{ij}$ now represents a signed Boolean matrix and,

$$d(Z_R) = d\left(R + \frac{K}{i\omega}\right). \tag{20}$$

Substituting $d(\mathbf{Z}_R)$ for the scaled single entry/Boolean matrix $\mathbf{P}_{ij}d(Z_R)$ Eq. 16 becomes,

$$d(Q) = \bar{\mathbf{f}}^{\mathrm{H}}\mathbf{Y}_C^{\mathrm{H}}\left(\left(\mathbf{P}_{ij}\mathbf{S} - \mathbf{P}_{ij}\mathbf{Y}_C^{\mathrm{H}}\mathbf{Y}_R^{-\mathrm{H}}\mathbf{S}\right)d(Z_R^*) - \mathbf{Y}_R^{-\mathrm{H}}\mathbf{S}\mathbf{Y}_C\mathbf{P}_{ij}d(Z_R)\right)\mathbf{Y}_C\bar{\mathbf{f}}. \tag{21}$$

Eq. 21 describes the change in complex power due to a small (complex) modification of the receiver at or between the ith and jth DoFs. From Eq. 21 we can identify two sensitivity relations:

$$\left.\frac{\partial Q}{\partial Z_R}\right|_{ij} = -\bar{\mathbf{f}}^{\mathrm{H}}\mathbf{Y}_C^{\mathrm{H}}\mathbf{Y}_R^{-\mathrm{H}}\mathbf{S}\mathbf{Y}_C\mathbf{P}_{ij}\mathbf{Y}_C\bar{\mathbf{f}} \tag{22}$$

and

$$\left.\frac{\partial Q}{\partial Z_R^*}\right|_{ij} = \bar{\mathbf{f}}^{\mathrm{H}}\mathbf{Y}_C^{\mathrm{H}}\left(\mathbf{P}_{ij}\mathbf{S} - \mathbf{P}_{ij}\mathbf{Y}_C^{\mathrm{H}}\mathbf{Y}_R^{-\mathrm{H}}\mathbf{S}\right)\mathbf{Y}_C\bar{\mathbf{f}}. \tag{23}$$

The above relations describe the sensitivity of the complex power Q with respect to a complex structural modification and its conjugate. It is, however, more convenient to express the above in terms of the real and imaginary parts, as opposed to complex conjugates. This can be achieved using the following set of equations [29,30]:

$$\begin{aligned} \frac{\partial \Re(Q)}{\partial \Re(Z_R)} &= \Re(A+B), \quad \frac{\partial \Re(Q)}{\partial \Im(Z_R)} = \Im(-A+B) \\ \frac{\partial \Im(Q)}{\partial \Re(Z_R)} &= \Im(A+B), \quad \frac{\partial \Im(Q)}{\partial \Im(Z_R)} = -\Re(-A+B) \end{aligned} \tag{24}$$

where $\Re(\;)$ and $\Im(\;)$ denote real and imaginary parts, respectively, and A and B are given by Eq. 22 and 23.

The sensitivity of the transmitted (real) power due to the application of a reactive structural modification (i.e. additional mass and/or stiffness) is then,

$$\begin{aligned} \left.\frac{\partial \Re(Q)}{\partial \Im(Z_R)}\right|_{ij} &= \Im(-A+B) \\ &= \Im\left(\bar{\mathbf{f}}^{\mathrm{H}}\mathbf{Y}_C^{\mathrm{H}}\mathbf{Y}_R^{-\mathrm{H}}\mathbf{S}\mathbf{Y}_C\mathbf{P}_{ij}\mathbf{Y}_C\bar{\mathbf{f}} + \bar{\mathbf{f}}^{\mathrm{H}}\mathbf{Y}_C^{\mathrm{H}}\left(\mathbf{P}_{ij}\mathbf{S} - \mathbf{P}_{ij}\mathbf{Y}_C^{\mathrm{H}}\mathbf{Y}_R^{-\mathrm{H}}\mathbf{S}\right)\mathbf{Y}_C\bar{\mathbf{f}}\right) \\ &= \Im\left(\bar{\mathbf{f}}^{\mathrm{H}}\mathbf{Y}_C^{\mathrm{H}}\left[\mathbf{Y}_R^{-\mathrm{H}}\mathbf{S}\mathbf{Y}_C\mathbf{P}_{ij} + \left(\mathbf{P}_{ij}\mathbf{S} - \mathbf{P}_{ij}\mathbf{Y}_C^{\mathrm{H}}\mathbf{Y}_R^{-\mathrm{H}}\mathbf{S}\right)\right]\mathbf{Y}_C\bar{\mathbf{f}}\right) \\ &= \Im\left(\bar{\mathbf{f}}^{\mathrm{H}}\mathbf{Y}_C^{\mathrm{H}}\left[\mathbf{Y}_R^{-\mathrm{H}}\mathbf{S}\mathbf{Y}_C\mathbf{P}_{ij} + \mathbf{P}_{ij}\left(\mathbf{I} - \mathbf{Y}_C^{\mathrm{H}}\mathbf{Y}_R^{-\mathrm{H}}\right)\mathbf{S}\right]\mathbf{Y}_C\bar{\mathbf{f}}\right). \end{aligned} \tag{25}$$

Similarly, considering the sensitivity of the transmitted (real) power due to the application of a resistive structural modification (i.e. additional damping),

$$\begin{aligned} \left.\frac{\partial \Re(Q)}{\partial \Re(Z_R)}\right|_{ij} &= \Re(A+B) \\ &= \Re\left(-\bar{\mathbf{f}}^{\mathrm{H}}\mathbf{Y}_C^{\mathrm{H}}\mathbf{Y}_R^{-\mathrm{H}}\mathbf{S}\mathbf{Y}_C\mathbf{P}_{ij}\mathbf{Y}_C\bar{\mathbf{f}} + \bar{\mathbf{f}}^{\mathrm{H}}\mathbf{Y}_C^{\mathrm{H}}\left(\mathbf{P}_{ij}\mathbf{S} - \mathbf{P}_{ij}\mathbf{Y}_C^{\mathrm{H}}\mathbf{Y}_R^{-\mathrm{H}}\mathbf{S}\right)\mathbf{Y}_C\bar{\mathbf{f}}\right) \\ &= \Re\left(\bar{\mathbf{f}}^{\mathrm{H}}\mathbf{Y}_C^{\mathrm{H}}\left[-\mathbf{Y}_R^{-\mathrm{H}}\mathbf{S}\mathbf{Y}_C\mathbf{P}_{ij} + \left(\mathbf{P}_{ij}\mathbf{S} - \mathbf{P}_{ij}\mathbf{Y}_C^{\mathrm{H}}\mathbf{Y}_R^{-\mathrm{H}}\mathbf{S}\right)\right]\mathbf{Y}_C\bar{\mathbf{f}}\right) \\ &= \Re\left(\bar{\mathbf{f}}^{\mathrm{H}}\mathbf{Y}_C^{\mathrm{H}}\left[-\mathbf{Y}_R^{-\mathrm{H}}\mathbf{S}\mathbf{Y}_C\mathbf{P}_{ij} + \mathbf{P}_{ij}\left(\mathbf{I} - \mathbf{Y}_C^{\mathrm{H}}\mathbf{Y}_R^{-\mathrm{H}}\right)\mathbf{S}\right]\mathbf{Y}_C\bar{\mathbf{f}}\right). \end{aligned} \tag{26}$$

By varying the ij indices of $\mathbf{P}_{ij}$, Eq. 25 and 26 can be used to identify the DoFs at which a small local or distributed modification will have the greatest influence on the transmitted power. This information can be used to design an optimum structural modification for reduced power flow.

3.1. Change in transmitted power

Once the power sensitivity has been determined it can be used to identify the most effective location to apply a structural modification. Following this, estimates can be made for the change in transmitted power,

$$\Delta\Re(Q) \approx \left.\frac{\partial \Re(Q)}{\partial \Im(Z_R)}\right|_{ij} \Im(\Delta Z_{ij}) + \left.\frac{\partial \Re(Q)}{\partial \Re(Z_R)}\right|_{ij} \Re(\Delta Z_{ij}) \tag{27}$$

At this point the structural modification ΔZ_{ij} can be optimised to achieve maximum reduction in transmitted power.

4. Numerical studies

In this section we present a numerical example demonstrating the application of the sensitivity relations derived above.

We consider a simple source-receiver system; two beams coupled end-to-end as illustrated in Fig. 2. The beams are modelled by FE and are represented by their free interface mobilities; the source beam is characterised by its interface mobility matrix $\mathbf{Y}_{Scc} \in \mathbb{C}^{2\times 2}$ where the two DoFs are a vertical translation and a cor-

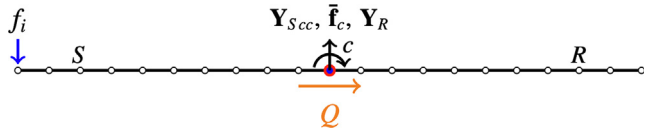

Fig. 2. Numerical coupled beam-beam model.

responding rotation, and the receiver is characterised by its full mobility matrix $\mathbf{Y}_R \in \mathbb{C}^{22\times22}$, which includes the interface DoFs alongside 20 remote DoFs (translations and rotations at 10 positions). Each beam was modelled with the material properties, $\rho = 7000$ kg/m^3, $E = 200\times10^9$ Pa, $\eta = 0.1$, and geometry $l_S = 0.4$ m, $l_R = 0.7$ m, $w_S = w_R = 0.05$ m and $h_S = h_R = 0.01$ m.

The source beam is excited internally by an 1 N force f_i, representing the unknown operational forces present in a typical vibration source. As per the component-based paradigm, the source activity (i.e. due to this internal force) is represented by the blocked force obtained at its coupling interface. Based on the component-level quantities described above, the complex power can be calculated as per Eq. 7.

Examples of the translational blocked force ($\bar{\mathbf{f}}_c$) and component mobilities ($\mathbf{Y}_S$ and $\mathbf{Y}_R$) are shown in Fig. 3a and b. The real (transmitted) and imaginary (oscillating) power Q is shown in Fig. 3c.

4.1. Finite difference verification

We begin by verifying the sensitivity expressions and inspecting their form. Verification is achieved by comparison against a finite difference approximation.

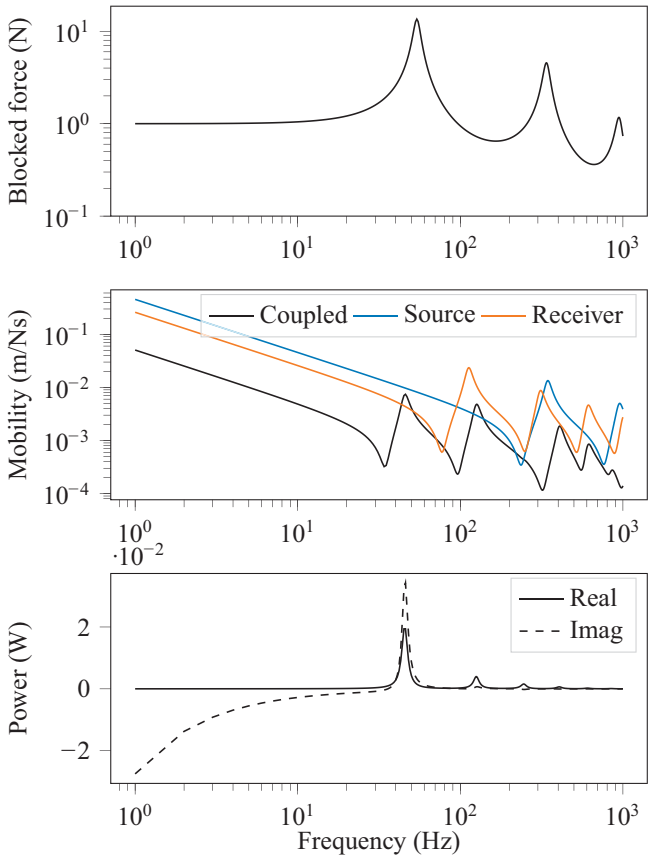

Fig. 3. Top - translational blocked force at interface of source due to a 1 N internal force. Middle - translational point mobility at interface for coupled assembly and uncoupled source and receiver. Bottom - real (transmitted) and imaginary (stored) power at the interface due to 1 N internal force.

For the local resistive modification this is achieved by adding a factor of 10^{-2} to the real part of the translational impedance at the interface DoF (index 0),

$$\mathbf{Z}_{R\Delta} = \mathbf{Z}_R + \mathbf{P}_{0,0}\times10^{-2} \tag{28}$$

computing the power Q_Δ, and then approximating the sensitivity as per,

$$\frac{\partial\Re(Q)}{\partial\Re(Z_R)}\Big|_{0,0} \approx \frac{\Re(Q_\Delta - Q)}{10^{-2}}. \tag{29}$$

For the reactive modification we use instead,

$$\mathbf{Z}_{R\Delta} = \mathbf{Z}_R + i\mathbf{P}_{0,0}\times10^{-2}. \tag{30}$$

The resulting comparisons are shown in Fig. 4.

For the distributed resistive modification we again add a factor of 10^{-2} to the real part of the translational impedance, this time including both an interface and remote DoF (indices 0 and 10),

$$\mathbf{Z}_{R\Delta} = \mathbf{Z}_R + \mathbf{P}_{0,10}\times10^{-2} \tag{31}$$

where $\mathbf{P}_{0,10}\times10^{-2}$ now includes off-diagonal coupling terms (see Eq. 21). The power Q_Δ is computed and the sensitivity approximated as per,

$$\frac{\partial\Re(Q)}{\partial\Re(Z_R)}\Big|_{0,10} \approx \frac{\Re(Q_\Delta - Q)}{10^{-2}}. \tag{32}$$

For the distributed reactive modification we use instead,

$$\mathbf{Z}_{R\Delta} = \mathbf{Z}_R + i\mathbf{P}_{0,10}\times10^{-2}. \tag{33}$$

The resulting comparisons are shown in Fig. 5.

Figs. 4 and 5 verify the local and distributed sensitivity relations presented above. Positive sensitivity values indicate that a positive modification (e.g. additional damping $Z_\Delta = R$ or mass $Z_\Delta = i\omega M$) will increase the transmitted power. A negative sensitivity indicates a reduction in transmitted power. For an added stiffness, the resulting impedance change is negative (e.g. $Z_\Delta = K/i\omega = -iK/\omega$) and so the interpretation of the sensitivity

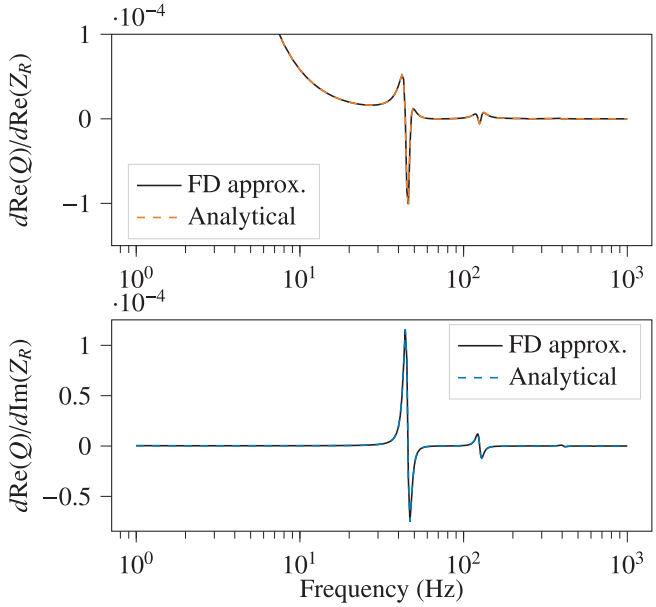

Fig. 4. Top - transmitted power sensitivity wrt. local resistive modification; dashed line - Eq. 26, solid line obtained by finite difference approximation. Bottom - transmitted power sensitivity wrt. local reactive modification; dashed line - Eq. 25, solid line obtained by finite difference approximation.

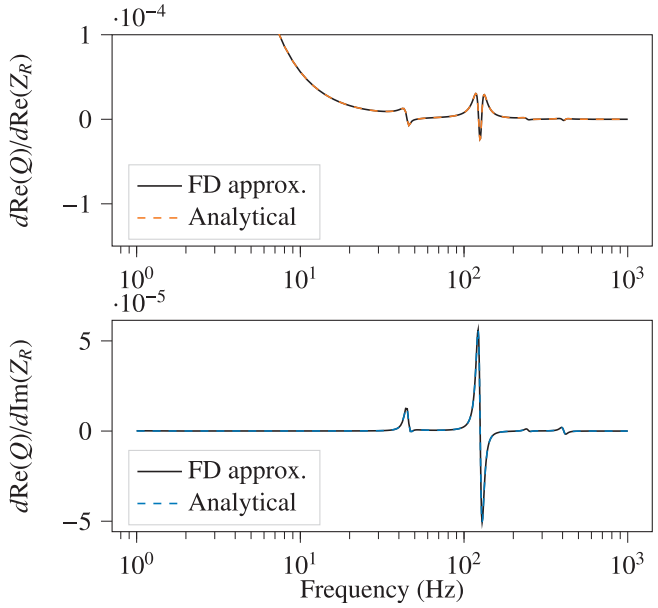

Fig. 5. Top - transmitted power sensitivity wrt. distributed resistive modification; dashed line - Eq. 26, solid line obtained by finite difference approximation. Bottom - transmitted power sensitivity wrt. distributed reactive modification; dashed line - Eq. 25, solid line obtained by finite difference approximation.

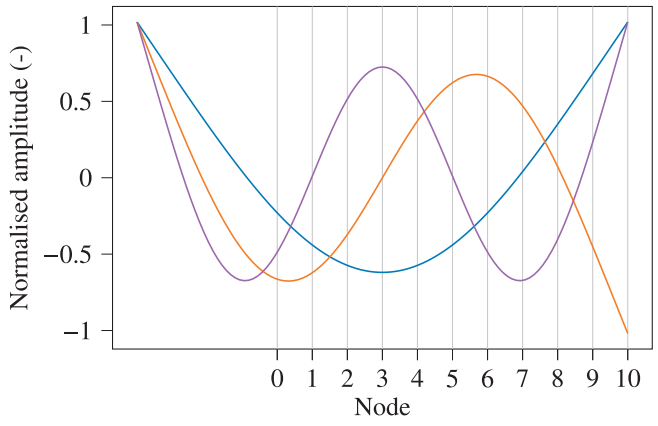

Fig. 6. First three modes of beam-beam system with labelled node positions (0 being the interface).

above is reversed; a negative sensitivity indicates an increase in power, and positive sensitivity a decrease in power.

A sensitivity peak followed by a trough indicates that for a positive impedance modification we get a downward shift in the resonant frequency of the structure and therefore the frequency of maximum transmitted power. This is an expected result. An 'M' shaped trend indicates a lowering of the peak transmitted power through a broadening of the resonance. i.e. energy is spread across neighbouring frequencies.

Comparing local vs distributed modifications, we see that the power sensitivity has changed considerably. For a distributed modification the second resonance has become the most sensitive to structural modification. This result suggests that by selecting which DoFs a modification is applied between, the effectiveness of a modification can be targeted towards a particular mode.

4.2. Influence of modification location

Having verified the sensitivity relations and considered the interpretation of their form, we can investigate the influence of their

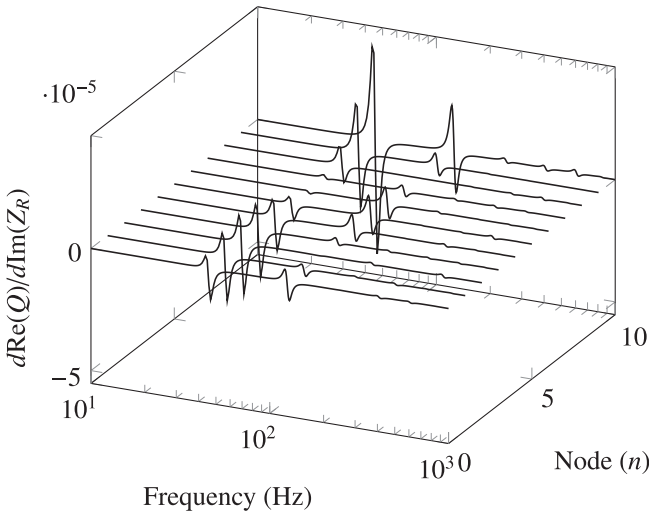

Fig. 7. Transmitted power sensitivity wrt. local reactive modification at the *n*th nodal point.

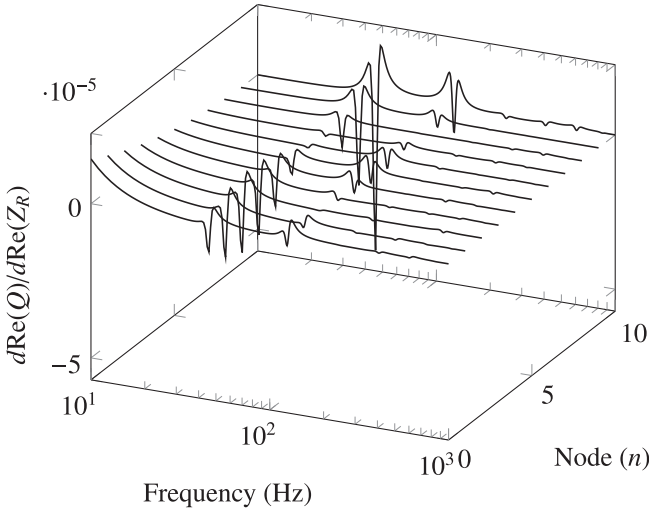

Fig. 8. Transmitted power sensitivity wrt. local resistive modification at the *n*th nodal point.

location on power flow sensitivity. For the simple beam-like structure considered here, the results presented below are somewhat expected. However, such expectations are limited to structures of simple form, whilst the sensitivity relations are general and can be applied to arbitrarily complex systems where intuition fails us.

We begin by considering local modifications of both resistive and reactive form. Shown in Fig. 7 and 8 are the power flow sensitivities obtained as we move the modification between the coupling interface (node 0) and the beam end (node 10), considering only the translational DoFs. From Figs. 7 and 8 it is seen that a maximum change in power for the first and second mode is achieved when a resistive modification (e.g. a grounded damper) is applied to the endmost node. This corresponds to the position of maximum deflection (see Fig. 6). In contrast, application of either modification to the 7th node has a minimal effect. As expected, this location corresponds to a region of small deflection.

Shown in Fig. 9 and 10 are the (resistive and reactive) sensitivities obtained for distributed modifications between the 0*th* (i.e. interface) DoF and the remaining nodes. Note that the 0 node trace is equivalent to the 0 node local modification in Figs. 7 and 8.

It is shown that for both resistive and reactive modifications we are able to obtain a much greater sensitivity (and therefore more

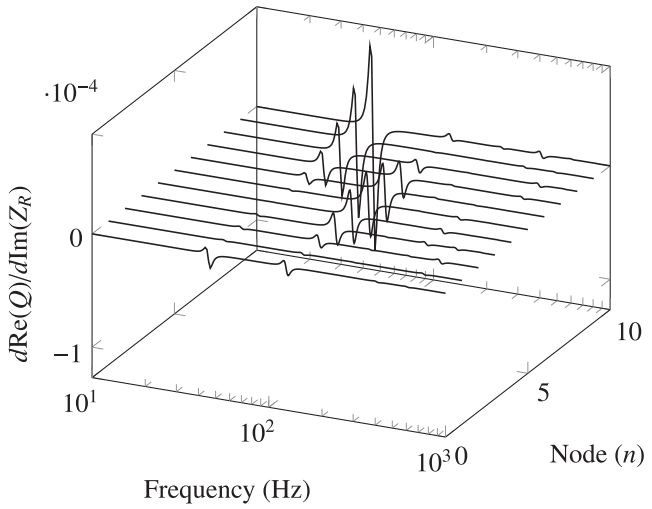

Fig. 9. Transmitted power sensitivity wrt. distributed reactive modification between the interface and nth nodal point.

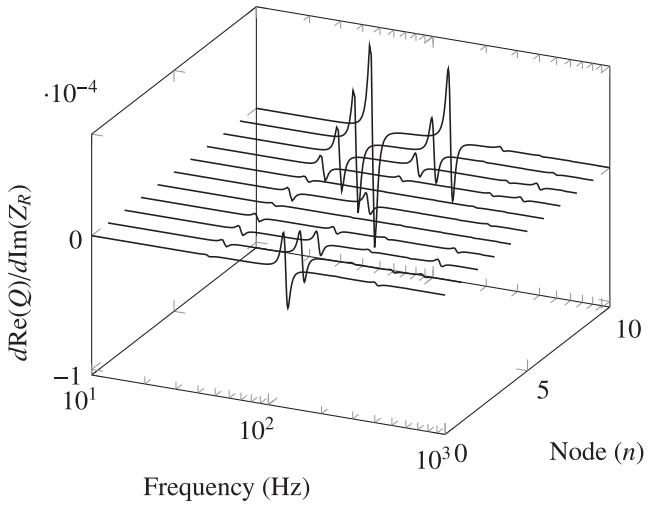

Fig. 11. Transmitted power sensitivity wrt. distributed reactive modification between the 5th and nth nodal point.

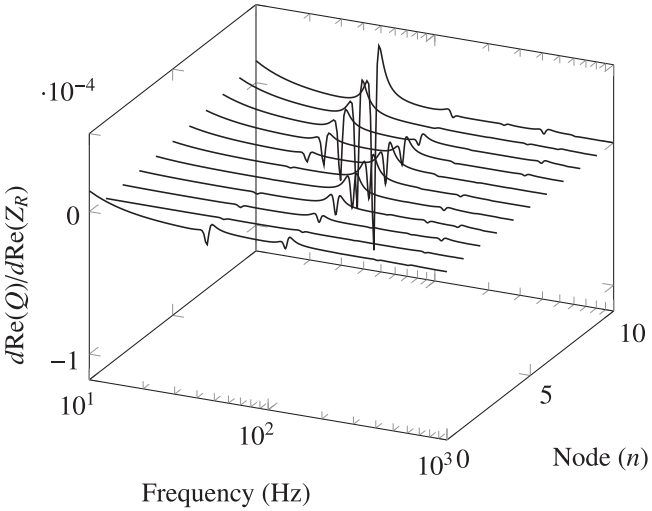

Fig. 10. Transmitted power sensitivity wrt. distributed reactive modification between the interface and nth nodal point.

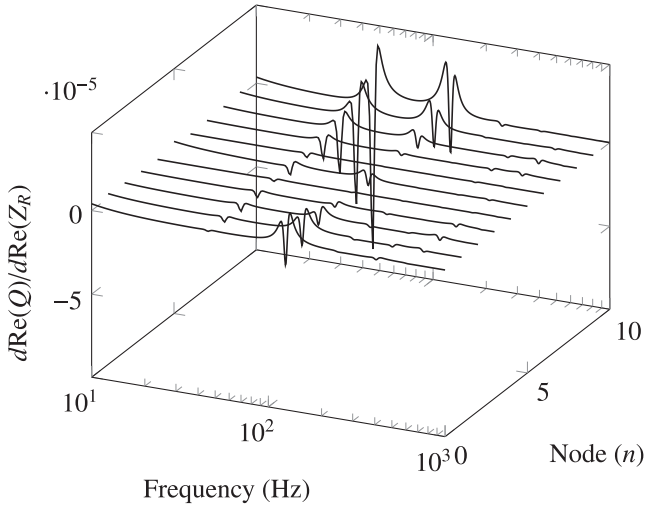

Fig. 12. Transmitted power sensitivity wrt. distributed reactive modification between the 5th and nth nodal point.

optimal modification) by using a distributed modification. As for a local modification, the sensitivity of a distributed modification appears proportional to the relative deflection between the two nodes of the modification. This can be seen by inspecting the node 10 trace of Figs. 9 or 10 and comparing the relative deflections of modes 1 and 2 (Fig. 6). Mode 1 shows a large relative deflection between nodes 0 and 10 with a normalised amplitude in excess of 1, whilst mode 2 remains less than 0.5. The sensitivities of modes 1 and 2 mirror this result. In contrast, the relative deflection between nodes 0 and 6 suggests large sensitivity for mode two and a low sensitivity for mode 1. These results are confirmed by Figs. 9 and 10.

Shown in Figs. 11 and 12 are the sensitivities obtained when treating node 5 as the fixed end of the modification. They further confirm the main conclusion of this numerical study; *power flow sensitivities are proportional to the relative deflection between the two ends of the modification.* Though this result is somewhat intuitive, for a complex structure it is not immediately obvious which of the modifiable DoFs is optimal. The proposed sensitivity relations provide a means of identifying, without need for intuition, the optimal DoFs for modification.

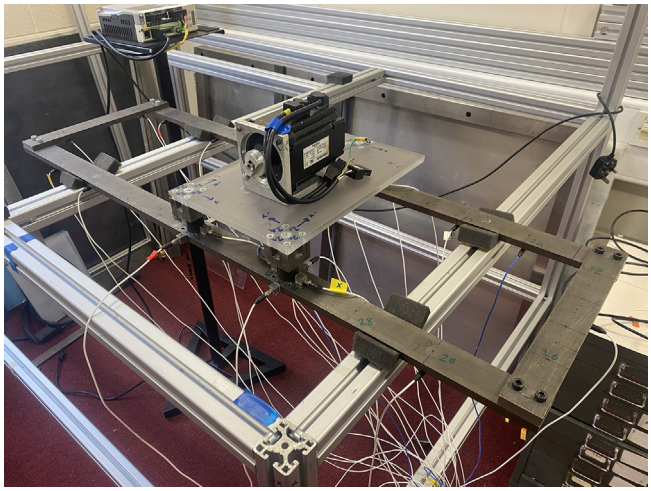

Fig. 13. Photo of experimental test rig.

5. Experimental case study

In this section we investigate the application of the proposed sensitivity analysis to an experimental case-study. The system understudy is shown in Fig. 13. It consists of a 3 footed vibration source (a perspex plate with an attached servo-motor) coupled resiliently to a steel frame-like receiver structure. To determine the transmitted power, and its sensitivity to structural modification, blocked forces are first identified at the base of each resilient coupling (such that the coupling elements are considered part of the source, and the frame alone is considered the receiver structure) using the in-direct method outlined in Section 2. The blocked force identification uses only response measurements made at the interface such that Eq. 3 takes the form,

$$\mathbf{v}_c = \mathbf{Y}_{Ccc}\bar{\mathbf{f}}_c \tag{34}$$

from which $\bar{\mathbf{f}}_c$ is determined by matrix inversion. Due to the highly resonant characteristics of the assembly, some regularisation is introduced to alleviate issues of ill-conditioning at certainty frequencies. A singular value discarding scheme was adopted, whereby any singular values λ_n below a threshold of $0.02 \times \max(\lambda)$ were set to zero. This threshold was obtained through trial and error by comparing measured and reconstructed (using blocked force) responses.

Each interface connection is initially represented by 4 translational z DoFs, spaced about the resilient coupling attachment point, as illustrated in Fig. 14. These 4 DoFs are transformed using the Finite Difference (FD) method [31] to obtain the translational z and rotational x/y DoFs at the centre of each connection point. In-plane x/y and rotational z DoFs were neglected. This was justified as previous works on a similar assembly have show that such a resiliently coupled system transmits vibration primarily through vertical translations, with x/y rotations becoming important at higher frequencies [22].

As required by Eq. 7 and 25–26, the uncoupled receiver mobility $\mathbf{Y}_R$ is also measured, using the same interface representation described above. In addition to the 12 interface DoFs (9 after the FD transformation), a further 11 translational z DoFs are included across the receiver structure. These are included to investigate the effect of a modification's position on the power flow sensitivity.

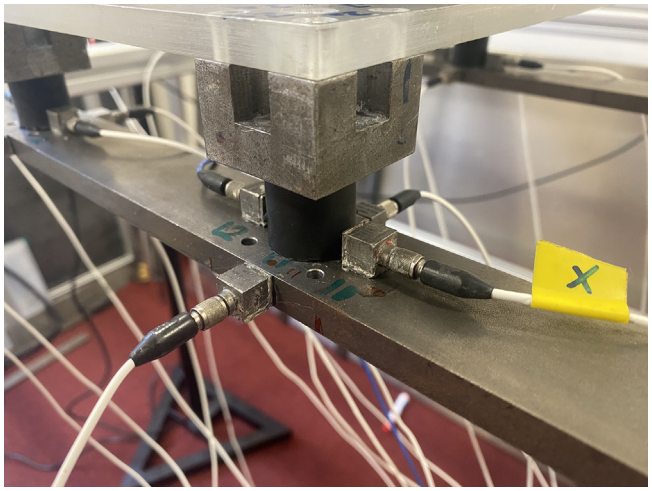

Fig. 14. Photo of interface instrumentation.

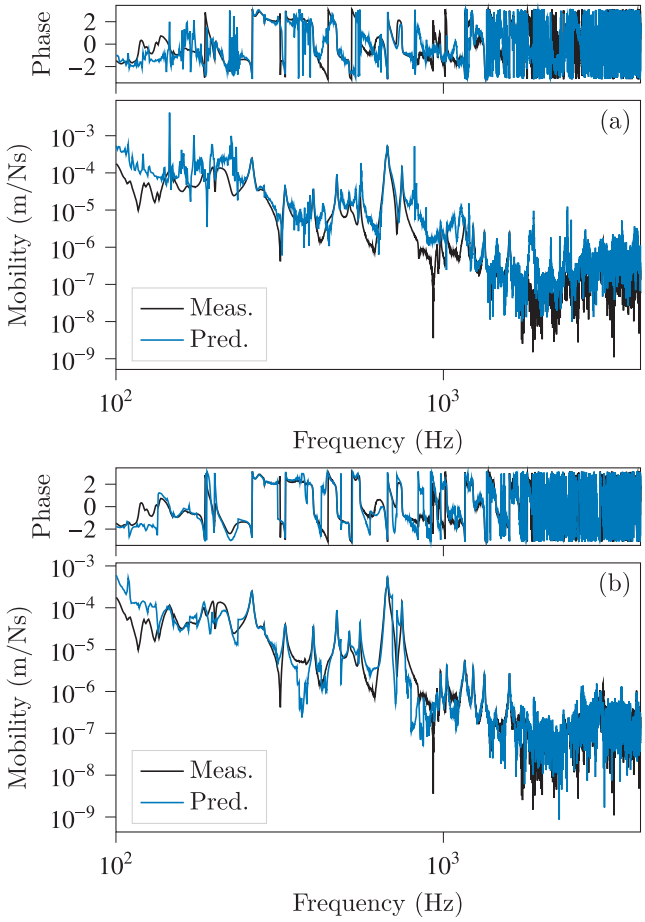

Fig. 15. On-board validation of blocked force without (a) and with (b) regularisation.

5.1. Blocked force and complex power

Shown in Figs. 15a and 15b are the on-board validation results of the blocked force (a response prediction made using the blocked

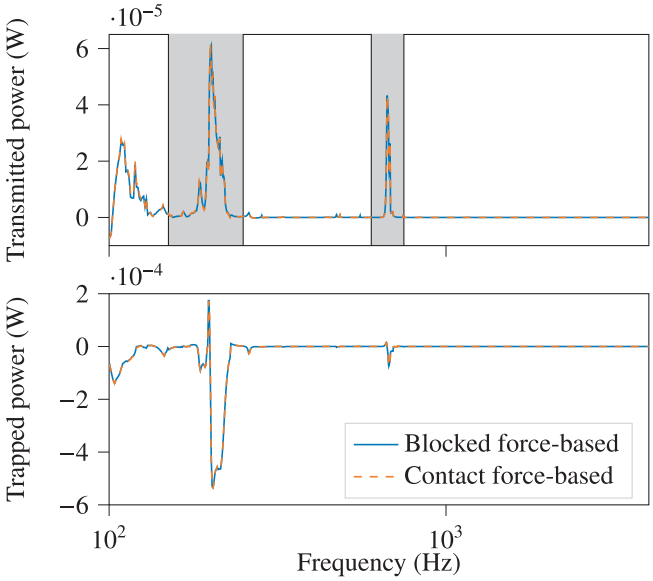

Fig. 16. Complex power (top - real, bottom - imaginary) obtained using the blocked force (Eq. 7) and contact force (Eq. 4).

force, compared against a direct measurement) obtained without and with the aforementioned regularisation, respectively. It is clear that the applied regularisation improves the overall agreement. This regularisation scheme is applied to all matrix inversion required hereafter. Above 2 kHz we begin to see the effect of instrumentation noise floor; this is due to the resilient coupling attenuating high frequencies.

Shown in Fig. 16 are the real (top) and imaginary (bottom) parts of the complex power obtained using the invariant blocked force (blue, using Eq. 7) and the contact force (orange, using Eq. 4). As expected, the two formulation for complex power yield near identical results. Highlighted in grey are two frequency ranges that demonstrate considerable power flow. These ranges will be subject to the proposed sensitivity analysis to determine optimum structural modifications.

5.2. Power flow sensitivity

Having determined the complex power flow through the interface, we are interested in identifying the optimum location and type of structural modification required to reduce the transmitted power. We apply Eqs. 27 and 28 across the two frequency ranges highlighted in Fig. 16. Fig. 17 corresponds to the frequency range 150–250 Hz, with a) showing the power flow sensitivity due to a local resistive modification, and b) a local reactive modification. Fig. 18 corresponds to the frequency range 600–750 Hz, with a) and b) similarly representing resistive and reactive modifications, respectively.

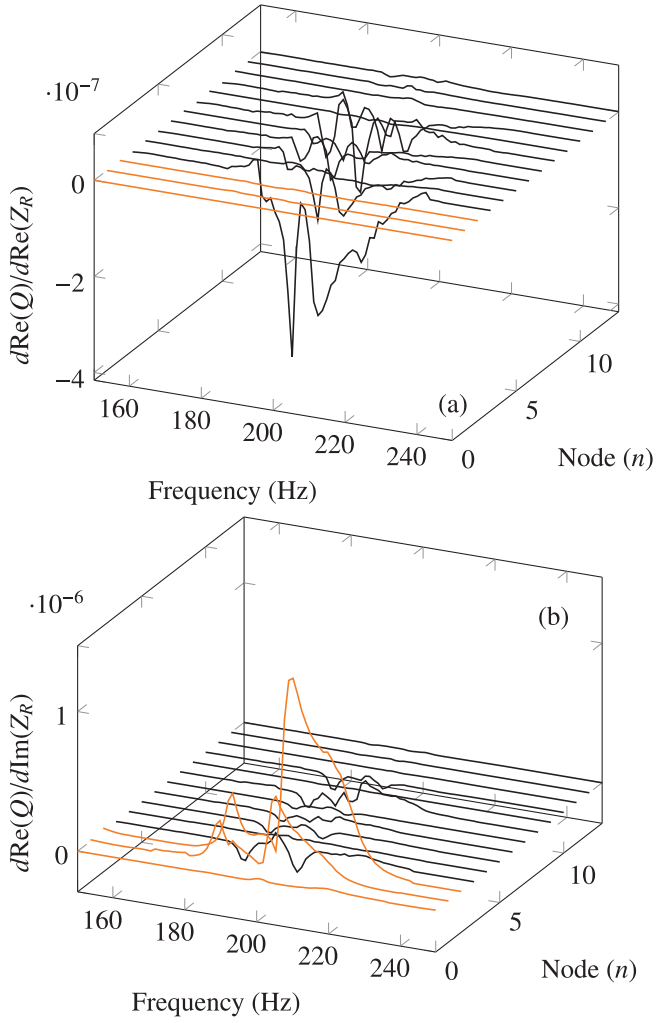

Fig. 17. Power flow sensitivity over the frequency range 150–250 Hz due to local resistive (a) and reactive (b) modifications at different measurement positions (n).

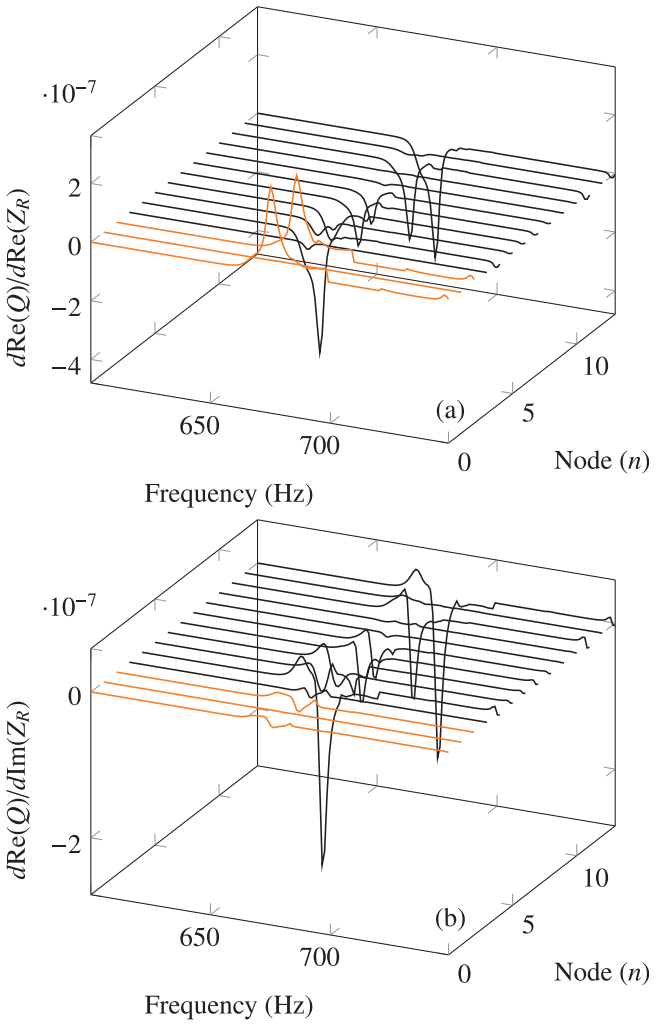

Fig. 18. Power flow sensitivity over the frequency range 600–750 Hz due to local resistive (a) and reactive (b) modifications at different measurement positions.

A total of 14 potential modification positions (nodes) are considered (these are included in the measurement of $\mathbf{Y}_C$ and $\mathbf{Y}_R$). Nodes 1–3 are the translational z interface DoFs (corresponding sensitivities are plot in orange), nodes 4–14 (also translational z) are spread over the receiver structure.

The results of Fig. 17 indicate that the greatest change in transmitted power is obtained by a reactive modification of the 3rd interface DoF. To reduce the transmitted power, this reactive modification should yield a negative modification impedance, i.e. it should be an added stiffness. If only a resistive modification were possible, Fig. 17a indicates that applying this to the interface would have little effect. Rather, node 4 would see the greatest reduction in power.

The results of Fig. 18 indicate that the greatest change in transmitted power between 600–750 Hz is obtained through modification of nodes 5 and 14, and that this is the case irrespective of whether the modification is resistive or reactive. Interestingly, Fig. 18a suggests that a resistive modification to the interface nodes 1 and 3 would in fact be detrimental, causing an increase in transmitted power. This sort of unexpected result gives reason to using a sensitivity-based analysis, such as Eqs. 25 and 26, to determine an optimum structural modification, as opposed to intuition.

6. Conclusions

Structural modifications can be used to reduce the power transmitted from vibrating machinery to connected receiver structures. An optimal structural modification, defined here as one that provides a large reduction in transmitted power for a minimal change in the dynamics of the receiver structure, is beneficial in many circumstances. We can identify an optimal modification by considering the derivative (i.e. sensitivity) of transmitted power, with respect to the impedance of the receiver structure. To this end, we derive a pair of sensitivity Eqs. 27 and 28, relating the real part of complex power (i.e. transmitted power) to resistive and reactive modifications of the receiver. An important advantage of the proposed sensitivity relations is that they are derived in terms of component-level quantities, meaning the analysis can be extended to virtual systems which do not necessarily exist physically. The sensitivity relations enable analysis of both local (e.g. where added mass or grounded stiffness/damping is applied to a single DoF) and distributed (e.g. where added stiffness/damping is applied between two DoFs) modifications. An arbitrary number of modification DoFs can be considered in the analysis, including both interface and remote positions. Rank ordering of the resulting sensitivities can be used to determine which DoF, when modified, will yield the greatest change in transmitted power. From this information, more focused optimisations studies could be used to design bespoke modifications for an even greater reduction in transmitted power.

Based on an in-direct force estimation, the proposed method is subject to the same limitations and sources of error. In fact, the presence of multiple matrix inversions in the resulting expressions, likely means that the sensitivity relations themselves have an increased susceptibility to experimental error.

Numerical studies on a coupled beam-beam structure verify the theory and provide some interpretation of the sensitivity plots. In general, it is observed that the greatest change in power is obtained when the relative deflection between the two ends of a modification is at a maximum. An experimental case study utilising a simple vibration source further demonstrates the application the sensitivity relations. It illustrates how the optimal modification position to reduce power flow depends on both frequency and the type of modification considered, e.g. the optimal location for added stiffness might have no effect if a damping modification is used instead. Furthermore, it demonstrates the presence of perhaps unintuitive results, such as an increase in power flow by adding damping to an interface.

In summary, the proposed sensitivity analysis for structural power flow provides a useful tool for vibro-acoustic design optimisation. It enables design engineers to make informed decisions with regards to optimal structural modifications, without having to rely on intuition which for complex problems is often unreliable.

CRediT authorship contribution statement

J.W.R. Meggitt: Conceptualization, Methodology, Validation, Investigation, Writing - original draft, Writing - review & editing.

Data availability

Data will be made available on request.

Declaration of Competing Interest

The authors declare that they have no known competing financial interests or personal relationships that could have appeared to influence the work reported in this paper.

References

[1] Goyder HGD, White RG. Vibrational power flow from machines into built-up structures, part i: Introduction and approximate analyses of beam and plate-like foundations. J Sound Vib 1980;68:59–75.
[2] Pinnington RJ, White RG. Power flow through machine isolators to resonanct and non-resonant beams. J Sound Vib 1981;75(2):179–97.
[3] Cuschieri JM. Structural power-flow analysis using a mobility approach of an l-shaped plate. J Acoust Soc Am 1990;87(3):1159–65.
[4] B. Petersson and B.M. Gibbs. Use of the source descriptor concept in studies of multi-point and multi-directional vibrational sources, 1993.
[5] Fulford RA, Gibbs BM. Structure-Borne Sound Power and Source Characterisation in Multi-Point-Connected Systems, Part 1: Case Studies for Assumed Force Distributions. J Sound Vib 1997;204(4):659–77.
[6] Moorhouse AT. On the characteristic power of structure-borne sound sources. J Sound Vib 2001;248(3):441–59.
[7] Sun L, Leung AYT, Lee YY, Song K. Vibrational power-flow analysis of a MIMO system using the transmission matrix approach. Mech Syst Signal Process Jan 2007;21(1):365–88.
[8] Van Der Seijs MV, De Klerk D, Rixen DJ. General framework for transfer path analysis: History, theory and classification of techniques. Mech Syst Signal Process 2016;68–69:217–44.
[9] Lyon RH, DeJong RG. the Development of Statistical Energy Analysis. 1995.
[10] Langley RS. A wave intensity technique for the analysis of high frequency vibrations. J Sound Vib 1992;159(3):483–502.
[11] Shorter PJ, Langley RS. On the reciprocity relationship between direct field radiation and diffuse reverberant loading. J Acoust Soc Am 2005;117(1):85.
[12] Hang H, Shankar K, Lai JCS. Prediction of the effects on dynamic response due to distributed structural modification with additional degrees of freedom. Mech Syst Signal Process 2008;22(8):1809–25.
[13] Young J, Myers K. Structure-borne sound power analysis for quantifying arbitrary structural modifications. J Sound Vib 2022;525:116749.
[14] Miller DW, Hall SR, Von Flotow AH. Optimal control of power flow at structural junctions. J Sound Vib 1990;140(3):475–97.
[15] Zhao Y, Wang Y, Ma W. Active control of power flow transmission in complex space truss structures based on the advanced timoshenko theory. J Vib Control 2015;21(8):1594–607.
[16] Done GTS, Hughes AD. Reducing vibration by structural modification. Vertica 1976;1(1):31–8.
[17] Sestieri A, D'ambrogio W. A modification method for vibration control of structures. Mech Syst Signal Process 1989;3(3):229–53.
[18] Young J, Myers K. Structure-borne power flow sensitivity analysis for general structural modifications. In: IMECE2021, San Fransisco.
[19] Moorhouse AT, Elliott AS, Evans TA. In situ measurement of the blocked force of structure-borne sound sources. Journal of Sound and Vibration 2009;325(4–5):679–85.
[20] International Organization for Standardization. ISO/NP 20270 Acoustics – Characterization of sources of structure-borne sound with respect to sound radiation from connected structures – Indirect in situ measurement of blocked forces at the contact points of machinery and equipment, 2017.
[21] Elliott AS, Moorhouse AT, Huntley T, Tate S. In-situ source path contribution analysis of structure borne road noise. J Sound Vib 2013;332(24):6276–95.
[22] Meggitt JWR, Moorhouse AT. On the completeness of interface descriptions and the consistency of blocked forces obtained in situ. Mech Syst Signal Process 2020;145:106850.
[23] Haeussler M, Mueller T, Pasma EA, Freund J, Westphal O, Voehringer T. Component tpa: Benefit of including rotational degrees of freedom and over-determination. In: Proceedings of the International Conference on Noise and Vibration Engineering Leuven, Belgium. p. 7–9.
[24] Prenant S, Padois T, Rolland V, Etchessahar M, Dupont T, Doutres O. Effects of mobility matrices completeness on component-based transfer path analysis methods with and without substructuring applied to aircraft-like components. J Sound Vib 2023;547:117541.
[25] M.W.F. Wernsen, M.V. Van Der Seijs, and D. de Klerk. An indicator sensor criterion for in-situ characterisation of source vibrations. In Conference Proceedings of the Society for Experimental Mechanics, number 5. Springer, 2017.
[26] Meggitt JWR, Elliott AS, Moorhouse AT. A covariance based framework for the propagation of uncertainty through inverse problems with an application to force identification. Mech Syst Signal Process 2018.
[27] Skudrzyk E. The foundations of acoustics: basic mathematics and basic acoustics. Springer Science & Business Media; 2012.
[28] Hjorunges A. Complex-Valued Matrix Derivatives. 1st edition,. Cambridge University Press; 2011.
[29] Meggitt JWR, Elliott AS, Moorhouse AT. A covariance based framework for the propagation of uncertainty through inverse problems with an application to force identification. Mech Syst Signal Process 2019;124:275–97.
[30] Meggitt JWR, Moorhouse AT. A covariance based framework for the propagation of correlated uncertainty in frequency based dynamic sub-structuring. Mech Syst Signal Process 2019.
[31] Elliott AS, Moorhouse AT, Pavić G. Moment excitation and the measurement of moment mobilities. J Sound Vib 2012;331(1):2499–519.